NORGES TEKNISK-NATURVITENSKAPELIGE
UNIVERSITET

Time-Symmetry of the Crouch–Grossman Method

by

Kenth Engø and Arne Marthinsen

PREPRINT
NUMERICS NO. 2/2000

NORWEGIAN UNIVERSITY OF SCIENCE AND
TECHNOLOGY
TRONDHEIM, NORWAY

This report has URL http://www.math.ntnu.no/preprint/numerics/2000/N2-2000.ps
Address: Department of Mathematical Sciences, Norwegian University of Science and Technology,
N-7491 Trondheim, Norway.

Time-Symmetry of the Crouch–Grossman Method

Kenth Engø*

Department of Informatics
University of Bergen
N-5020 Bergen
Norway

Arne Marthinsen†

Department of Mathematical Sciences
Norwegian University of Science and Technology
N-7491 Trondheim
Norway

23rd May 2000

Abstract

We study time-symmetry of the Crouch–Grossman method. We introduce and motivate the definition for the adjoint of an s-stage Crouch–Grossman method. Further, we show that the adjoint method can be analyzed as a Crouch–Grossman method with $2s-1$ stages. The increase in the number of stages for the adjoint method is a consequence of the non-commutativity of the elementary flows. Assuming the flows to be Abelian will reduce the proposed adjoint method to a Crouch–Grossman method based on the classical adjoint method of the underlying Runge–Kutta scheme. Examples of high-order symmetric (self-adjoint) Crouch–Grossman methods are also given. Properties of the methods are demonstrated with numerical experiments on the Sine–Euler equation and the heavy top equation.

Mathematics Subject Classification 2000: 65L06, 34C40

Key Words: Crouch–Grossman method, time-symmetry, adjoint method, symmetric method, Runge–Kutta method, geometric integration, numerical mathematics

*Email: `Kenth.Engo@ii.uib.no`, WWW: `http://www.ii.uib.no/~kenth/`

†Email: `Arne.Marthinsen@math.ntnu.no`, WWW: `http://www.math.ntnu.no/~arnema/`

1 Introduction

The Crouch–Grossman method was introduced by Crouch and Grossman in [2]. A thorough analysis of the method, in the setting usual for Runge–Kutta methods, was performed by Owren and Marthinsen [14], and also other papers discuss and analyze this method as a numerical integrator on Lie groups [13, 10, 12]. In this paper we want to focus on the issue of time-symmetry for the Crouch–Grossman method. Time-symmetric numerical integrators are advantageous in many applications, and we consider it important and necessary to investigate this property also for the family of Crouch–Grossman methods.

Our motivation for studying time-symmetry of Crouch–Grossman methods arose from the following observation. A Crouch–Grossman method advances the solution from time t_n to t_{n+1} through a composition of elementary flows in such a way that a Butcher tableau containing the method coefficients completely determines the integrator. By using the coefficients of the classical trapezoidal rule in the Crouch–Grossman setting and performing the interchanges $y_n \leftrightarrow y_{n+1}$ and $h \leftrightarrow -h$, as is common in classical theory for symmetric Runge–Kutta methods, we see that the Crouch–Grossman method remains the same. Numerical simulations also verify that the coefficients of the trapezoidal rule gives a method that is indeed symmetric, i.e. the numerical flow is centered at the midpoint along the exact flow. However, the coefficients of other classically symmetric methods did not lead to symmetric Crouch–Grossman methods. The general non-commutativity of the elementary flows is the reason why the classical results do not carry over to the Crouch–Grossman case.

When numerically integrating a differential equation, we want to approximate the integral curve obtained by applying the flow operator to the initial condition. One important property of the true flow operator is that it is selfadjoint; i.e., starting from an initial point on the manifold and advancing along the integral curve a time increment, and then reversing, will take you back to the initial point. The flow's selfadjointness – or time-symmetry (we will use the terms interchangeably) – is a property valid regardless of the domain the differential equation is evolving on. Hence, studying time-symmetry of numerical methods on manifolds is just as important as in the classical case, where the adjoint numerical method is a central tool. Time-symmetry of the Magnus expansion was shown in [9], while time-symmetric properties of the Runge–Kutta–Munthe-Kaas method and the generalized Magnus expansion for nonlinear differential equations were treated in [15].

The remainder of this paper is organized as follows: The next section discusses time-symmetry of Crouch–Grossman methods, and we develop the general form of the adjoint of any Crouch–Grossman method. We also show particular examples of symmetric Crouch–Grossman methods. In Section 3 we support the theoretical findings with numerical experiments. We end the paper with some concluding remarks.

2 Time-Symmetry of the Crouch–Grossman Method

Let $E_1, \dots, E_d$ be smooth vector fields that at each point p in a differentiable manifold $\mathcal{M}$ span the tangent space $\mathrm{T}_p\mathcal{M}$. Such a collection of vector fields is called a frame. A vector field relative to this frame can be written as $F(y) = \sum_{i=1}^{d} f_i(y)E_i$, where $f_i : \mathcal{M} \to \mathbb{R}$ are smooth functions. Initial value problems on the manifold can be expressed in terms of the frame as

$$y' = F(y) = \sum_{i=1}^{d} f_i(y) E_i \tag{1}$$

together with the initial condition $y(0) = y_0 \in \mathcal{M}$.

The exact solution of (1) is given as the flow of the vector field F through the initial point on the manifold. Computation of the exact flow of the vector field is in general not a feasible task, hence we look for suitable approximations. The Crouch–Grossman method is based on vector fields with frozen coefficients, which we denote by $F_p = \sum_{i=1}^{d} f_i(p) E_i$. Using exponentiation to denote the flow of a vector field, we can write the application of one step with a Crouch–Grossman method from y_n to y_{n+1} as follows:

$$\begin{aligned} Y_i &= \exp(ha_{i,s}F_{Y_s}) \exp(ha_{i,s-1}F_{Y_{s-1}}) \cdots \exp(ha_{i,1}F_{Y_1}) y_n, \qquad i = 1, \ldots, s, \\ y_{n+1} &= \exp(hb_s F_{Y_s}) \exp(hb_{s-1}F_{Y_{s-1}}) \cdots \exp(hb_1 F_{Y_1}) y_n. \end{aligned} \tag{2}$$

Here, the real number h is the stepsize. The notational extension to non-autonomous equations follows in the obvious way. The coefficients $a_{i,j}$ and b_i, and, in the case of non-autonomous equations, c_i, are normally presented in a Butcher tableau:

$$\begin{array}{c|ccc} c_1 & a_{1,1} & \cdots & a_{1,s} \\ \vdots & \vdots & & \vdots \\ c_s & a_{s,1} & \cdots & a_{s,s} \\ \hline & b_1 & \cdots & b_s \end{array} \tag{3}$$

Given a numerical method solving differential equations evolving on manifolds, we define its order of approximation as in [14]: the method is of order p if the p first terms of its Lie series are identical to the p first terms of the Lie series of the exact flow. The Lie series of the exact flow is given by

$$\begin{aligned} \Psi\big(\exp(hF)(m)\big) &= \Psi(m) + hF[\Psi](m) + \frac{h^2}{2} F^2[\Psi](m) + \cdots \\ &= \sum_{i=0}^{\infty} \frac{h^i}{i!} F^i[\Psi](m), \end{aligned}$$

where $m \in \mathcal{M}$, and Ψ is an arbitrary, real-valued, smooth function [14].

2.1 Adjoint Crouch–Grossman Methods

A fundamental geometric property of the flow φ_t of an autonomous differential equation

$$\frac{dy}{dt} = f(y), \qquad y(0) = y_0 \in \mathcal{M}, \tag{4}$$

is time-symmetry (also known as the flow, group, or adjoint property):

$$\varphi_{-t} \circ \varphi_t(y) = y. \tag{5}$$

The interpretation of (5) is obvious: Take y_0 as an initial point on the manifold $\mathcal{M}$ and follow the flow forwards in time an amount t to arrive at y_1. Starting in y_1 and going backwards in time $-t$, you end up in y_0.

In the numerical solution of the differential equation (4), the flow $\varphi_h : \mathcal{M} \to \mathcal{M}$ is approximated by a (one-step) numerical method $\Phi_h : \mathcal{M} \to \mathcal{M}$ with stepsize h. The time-symmetry property (5) is a basic property of the true flow, but is not necessarily shared by all numerical methods. Consider for instance the classical, explicit Euler method. Integrating (4) with stepsize h yields the approximation $y_1 = y_0 + hf(y_0)$. Now, taking y_1 as initial value and integrating backwards with stepsize $-h$ gives

$$\begin{aligned} y_0^* &= y_1 - hf(y_1) \\ &= y_0 + hf(y_0) - hf(y_0 + hf(y_0)) \\ &= y_0 - h^2 f(y_0) f'(y_0) + \mathcal{O}(h^3), \end{aligned}$$

which is different from y_0 in second order of h. Hence, the time-symmetry property is only retained up to the order of the method.

In the classical case [8, 7], in order to do a detailed analysis of time-symmetry, one has introduced the concept of adjoint numerical method Φ_h^*. We can adopt the same definition in the generalized manifold setting, as has been done in [15]: Given a numerical one-step method Φ_h, the adjoint method can be defined as

$$\Phi_h^* = \Phi_{-h}^{-1}, \tag{6}$$

inspired by the time-symmetry property (5). To calculate the adjoint method according to this definition, consider $y_1 = \Phi_h^*(y_0) = \Phi_{-h}^{-1}(y_0)$, which yields $y_0 = \Phi_{-h}(y_1)$. Thus, one way of calculating the adjoint method is by performing the interchanges $h \leftrightarrow -h$ and $y_0 \leftrightarrow y_1$ in the numerical method Φ_h, and solve for y_1. Returning to the example with Euler's method, it is easy to verify that the adjoint of the explicit Euler method is implicit Euler: $y_1 = y_0 + hf(y_1)$.

Based on (6), we will now go through an example for finding the form of the adjoint Crouch–Grossman method. The general 2-stage Crouch–Grossman method based on the coefficients

$$\begin{array}{c|cc} c_1 & a_{11} & a_{12} \\ c_2 & a_{21} & a_{22} \\ \hline & b_1 & b_2 \end{array}$$

is given as

$$\begin{aligned} Y_1 &= \exp(ha_{12}F_{Y_2}) \exp(ha_{11}F_{Y_1}) y_n \\ Y_2 &= \exp(ha_{22}F_{Y_2}) \exp(ha_{21}F_{Y_1}) y_n \\ y_{n+1} &= \exp(hb_2 F_{Y_2}) \exp(hb_1 F_{Y_1}) y_n. \end{aligned}$$

Performing the interchanges $y_n \leftrightarrow y_{n+1}$ and $h \leftrightarrow -h$, and substituting in for y_{n+1} in the stages, yields

$$\begin{aligned} Y_1 &= \exp(-ha_{12}F_{Y_2}) \exp\big(h(b_1 - a_{11})F_{Y_1}\big) \exp(hb_2 F_{Y_2}) y_n \\ Y_2 &= \exp(-ha_{22}F_{Y_2}) \exp\big(h(b_1 - a_{21})F_{Y_1}\big) \exp(hb_2 F_{Y_2}) y_n \\ y_{n+1} &= \exp(hb_1 F_{Y_1}) \exp(hb_2 F_{Y_2}) y_n. \end{aligned}$$

What is the most natural interpretation of the above? The non-commutativity of the elementary flows creates the problem that the rightmost flow cannot be swapped with the center flow in the stages. That is, however, accomplished in the classical commutative case, and one can see how the classical coefficient requirement arises. Now, in the non-commutative setting we are forced to renew our thinking.

One way to think about the obtained adjoint method, is to consider it as a Crouch–Grossman method with 3 stages. This is natural since the stages consist of composition of three flows, and this conforms with the general definition of a Crouch–Grossman method: the number of stages is equal to the number of elementary flows. It is clear from the above adjoint method that the order of appearance of the stages is reversed, and by introducing a dummy stage that equals the first stage, we get

$$\begin{aligned}
Y_2 &= \exp(-ha_{22}F_{Y_2})\exp\big(h(b_1-a_{21})F_{Y_1}\big)\exp(hb_2F_{Y_2})y_n\\
Y_1 &= \exp(-ha_{12}F_{Y_2})\exp\big(h(b_1-a_{11})F_{Y_1}\big)\exp(hb_2F_{Y_2})y_n\\
Y_2 &= \exp(-ha_{22}F_{Y_2})\exp\big(h(b_1-a_{21})F_{Y_1}\big)\exp(hb_2F_{Y_2})y_n\\
y_{n+1} &= \exp(hb_1F_{Y_1})\exp(hb_2F_{Y_2})y_n,
\end{aligned}$$

or, expressed in tableau form,

$$\begin{array}{c|ccc}
1-c_2 & b_2 & (b_1-a_{21}) & -a_{22}\\
1-c_1 & b_2 & (b_1-a_{11}) & -a_{12}\\
1-c_2 & b_2 & (b_1-a_{21}) & -a_{22}\\
\hline
 & b_2 & b_1 & 0
\end{array} \tag{7}$$

In general, a Crouch–Grossman method (2) with s stages and Butcher tableau (3) will give rise to an adjoint method with $2s-1$ stages. The Butcher tableau of the adjoint method is then, in general, expressible as:

$$\begin{array}{c|cccccccc}
1-c_s & b_s & b_{s-1} & \cdots & b_2 & b_1-a_{s,1} & -a_{s,2} & \cdots & -a_{s,s}\\
1-c_{s-1} & b_s & b_{s-1} & \cdots & b_2 & b_1-a_{s-1,1} & -a_{s-1,2} & \cdots & -a_{s-1,s}\\
\vdots & \vdots & \vdots & & \vdots & \vdots & \vdots & & \vdots\\
1-c_2 & b_s & b_{s-1} & \cdots & b_2 & b_1-a_{2,1} & -a_{2,2} & \cdots & -a_{2,s}\\
1-c_1 & b_s & b_{s-1} & \cdots & b_2 & b_1-a_{1,1} & -a_{1,2} & \cdots & -a_{1,s}\\
1-c_2 & b_s & b_{s-1} & \cdots & b_2 & b_1-a_{2,1} & -a_{2,2} & \cdots & -a_{2,s}\\
\vdots & \vdots & \vdots & & \vdots & \vdots & \vdots & & \vdots\\
1-c_{s-1} & b_s & b_{s-1} & \cdots & b_2 & b_1-a_{s-1,1} & -a_{s-1,2} & \cdots & -a_{s-1,s}\\
1-c_s & b_s & b_{s-1} & \cdots & b_2 & b_1-a_{s,1} & -a_{s,2} & \cdots & -a_{s,s}\\
\hline
 & b_s & b_{s-1} & \cdots & b_2 & b_1 & 0 & \cdots & 0
\end{array} \tag{8}$$

A first observation is the obvious symmetry in the coefficients. The first and the last line in the coefficient matrix coincide, and so do the second and second last line. In fact, the rows are symmetrically placed around row s. Note also that the $s-1$ rightmost weights are zero. This means that, although the adjoint system has $2s-1$ stages, the computation cost involved is comparable to what an s stage implicit method requires. Note also that the first $s-1$ entries of each row in the tableau are the same, hence the resulting product needs only be computed once and reused in the next $s-1$ stages.

To verify numerically that a Crouch–Grossman method based on this Butcher tableau is the adjoint of the one based on the tableau (3), we integrate the rigid body equations [3] by first taking a step of size $h/2$ with tableau (3) and then a step of size $h/2$ with (8). The governing equations are given by

$$\frac{\mathrm{d}y}{\mathrm{d}t} = y \times \mathcal{I}^{-1} y,$$

where $y \in \mathbb{R}^3$ is the momentum vector and $\mathcal{I} = \operatorname{diag}\left(\frac{7}{8}, \frac{5}{8}, \frac{1}{4}\right)$ is the inertia tensor. As initial condition we have used $y(0) = [0.875, 0.625, 0.250]$, and we integrate from $t_0 = 0$ to $t_{\text{end}} = 25$ with a stepsize of 0.1. Our main concern in these simulations is to verify that the resulting method is of even order. Figure 1 shows some of the results. The coefficients used in the simulations are the third order **CG3a** and the fourth order **CG4** from [14], and the fifth order **CG5a** from [10]. The methods composed with their adjoint give even order overall methods.

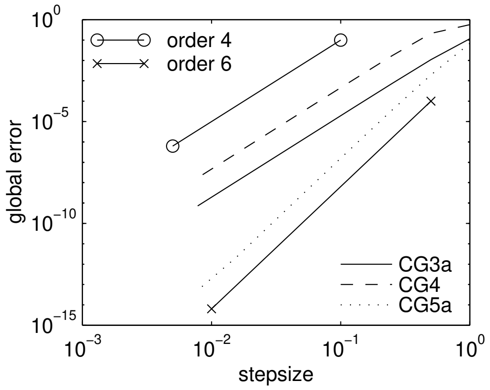

Figure 1: The figure shows the global error as a function of stepsize for integration using the method composed with its adjoint method. The methods are of order three, four and five, respectively. Both the third and the fourth order methods lead to an overall fourth order method, while the fifth order method leads to one of overall order six.

The above discussion can be summarized in the following theorem.

Theorem 2.1
Let $\exp(hX)(m)$ denote the flow of the smooth vector field X through $m \in \mathcal{M}$, and let $y' = X(y)$ with initial condition $y(0) = m$. Furthermore, let $\Psi \in C^\infty(\mathcal{M}, \mathbb{R})$, and let $\Phi_h : \mathcal{M} \to \mathcal{M}$ be a numerical method of order p, i.e. it satisfies

$$\Psi(\Phi_h(m)) = \Psi(\exp(hX)(m)) + Y[\Psi](m)h^{p+1} + \mathcal{O}(h^{p+2}), \tag{9}$$

where $Y[\Psi] \in C^\infty(\mathcal{M}, \mathbb{R})$ is an $(n+1)$-derivation of Ψ. Then the adjoint method $\Phi_h^* = \Phi_{-h}^{-1}$ has the same order p, and the identity

$$\Psi(\Phi_h^*(m)) = \Psi(\exp(hX)(m)) + (-1)^p Y[\Psi](m)h^{p+1} + \mathcal{O}(h^{p+2}) \tag{10}$$

holds.

A consequence of this theorem is that the numerical method $\Phi^*_{h/2} \circ \Phi_{h/2}$ is a method of even order. If Φ_h is symmetric, then its maximal order is even.

Proof: In order to find the adjoint method, we perform the swaps $h \leftrightarrow -h$ and $m \leftrightarrow \exp(hX)(m)$ in (9), and obtain

$$\Psi(\Phi_{-h}(\exp(hX)(m))) = \Psi(m) + Y[\Psi](\exp(hX)(m))(-h)^{p+1} + \mathcal{O}(h^{p+2}).$$

Since (9) is valid for any smooth function, it is in particular valid for $\Psi \circ \Phi^{-1}_{-h}$. Hence,

$$\begin{aligned}\Psi(\exp(hX)(m)) &= \Psi(\Phi^{-1}_{-h}(m)) \\ &\quad + (-1)^{p+1} Y[\Psi \circ \Phi^{-1}_{-h}](\exp(hX)(m))h^{p+1} + \mathcal{O}(h^{p+2}),\end{aligned}$$

which can be rearranged as

$$\begin{aligned}\Psi(\Phi^*_h(m)) &= \Psi(\exp(hX)(m)) \\ &\quad + (-1)^{p} Y[\Psi \circ \Phi^{-1}_{-h}](\exp(hX)(m))h^{p+1} + \mathcal{O}(h^{p+2}).\end{aligned} \tag{11}$$

Assuming backward error analysis [6], one can argue that

$$\Psi \circ \Phi^{-1}_{-h} = \Psi + h\Psi_1 + \frac{h^2}{2}\Psi_2 + \cdots . \tag{12}$$

Expanding $Y[\Psi \circ \Phi^{-1}_{-h}]\big(\exp(hX)(m)\big)$ into its Lie series $Y[\Psi \circ \Phi^{-1}_{-h}](m) + \mathcal{O}(h)$, and substituting this and (12) into (11), yields the desired result (10). □

We conclude this section with stressing the following fact: The known classical relation $\Phi = (\Phi^*)^*$ is still valid in the non-commutative setting. Despite the immediate increase in number of stages in $(\Phi^*)^*$, equality in the stages will reduce the effective number of stages down to the initial count in Φ.

2.2 Self-Adjoint Crouch–Grossman Methods

There are only a few examples of self-adjoint or symmetric Crouch–Grossman methods, i.e. methods that satisfy $\Phi_h = \Phi^{-1}_{-h}$, among the *known* Crouch–Grossman methods. Crouch–Grossman methods with only one stage ($s = 1$) coincide with the one-stage Runge–Kutta–Munthe-Kaas methods, and, as shown in [15], the method based on the coefficients of the implicit midpoint rule is self-adjoint. In Section 1 we pointed out that the 2-stage method based on the coefficients of the trapezoidal rule is symmetric. Showing this is straight forward. According to (8) the adjoint method of the trapezoidal rule is

$$\begin{array}{c|ccc} 0 & 1/2 & 0 & -1/2 \\ 1 & 1/2 & 1/2 & 0 \\ 0 & 1/2 & 0 & -1/2 \\ \hline & 1/2 & 1/2 & 0 \end{array}$$

In this scheme, the first and third stages collapse. By ignoring the last zero in the weights and in the second stage, we are back to the trapezoidal rule.

These two examples might indicate that as long as the underlying Runge–Kutta method is symmetric, so is the Crouch–Grossman method. However, numerical experiments refute a conclusion of this kind.

Constructing symmetric Crouch–Grossman methods by composition As for self-adjoint Crouch–Grossman methods of order greater than 2, we know that they exist. We will use an approach based on composition of two Crouch–Grossman methods in order to construct higher-order Crouch–Grossman methods. According to Theorem 2.1 we must search for an even-order method, and we exemplify the approach by constructing a forth-order symmetric method.

Take any s stage Crouch–Grossman method and compose it with its adjoint method of $2s-1$ stages. Then the composed method is a symmetric Crouch–Grossman method with $3s-1$ stages. Let us fix the number of stages to $s=3$:

$$\begin{array}{c|ccc} c_1 & a_{11} & a_{12} & a_{13} \\ c_2 & a_{21} & a_{22} & a_{23} \\ c_3 & a_{31} & a_{32} & a_{33} \\ \hline & b_1 & b_2 & b_3 \end{array}$$

Composing this Crouch–Grossman method with its adjoint method (8) yields the following 8-stage method:

$$\frac{1}{2}\cdot\left(\begin{array}{c|cccccccc} c_1 & a_{11} & a_{12} & a_{13} & 0 & 0 & 0 & 0 & 0 \\ c_2 & a_{21} & a_{22} & a_{23} & 0 & 0 & 0 & 0 & 0 \\ c_3 & a_{31} & a_{32} & a_{33} & 0 & 0 & 0 & 0 & 0 \\ 2-c_3 & b_1 & b_2 & b_3 & b_3 & b_2 & b_1-a_{31} & -a_{32} & -a_{33} \\ 2-c_2 & b_1 & b_2 & b_3 & b_3 & b_2 & b_1-a_{21} & -a_{22} & -a_{23} \\ 2-c_1 & b_1 & b_2 & b_3 & b_3 & b_2 & b_1-a_{11} & -a_{12} & -a_{13} \\ 2-c_2 & b_1 & b_2 & b_3 & b_3 & b_2 & b_1-a_{21} & -a_{22} & -a_{23} \\ 2-c_3 & b_1 & b_2 & b_3 & b_3 & b_2 & b_1-a_{31} & -a_{32} & -a_{33} \\ \hline & b_1 & b_2 & b_3 & b_3 & b_2 & b_1 & 0 & 0 \end{array}\right). \tag{13}$$

Based on the coefficients of the 3-stage, third order, explicit Crouch–Grossman method **CG3a** given in [14], we obtain a 4th order symmetric Crouch–Grossman method:

$$\begin{array}{c|cccccccc} 0 & 0 & 0 & 0 & 0 & 0 & 0 & 0 & 0 \\ 3/8 & 3/8 & 0 & 0 & 0 & 0 & 0 & 0 & 0 \\ 17/48 & 119/432 & 17/216 & 0 & 0 & 0 & 0 & 0 & 0 \\ 31/48 & 13/102 & -1/3 & 12/17 & 12/17 & -1/3 & -443/2993 & -17/216 & 0 \\ 5/8 & 13/102 & -1/3 & 12/17 & 12/17 & -1/3 & -101/408 & 0 & 0 \\ 1 & 13/102 & -1/3 & 12/17 & 12/17 & -1/3 & 13/102 & 0 & 0 \\ 5/8 & 13/102 & -1/3 & 12/17 & 12/17 & -1/3 & -101/408 & 0 & 0 \\ 31/48 & 13/102 & -1/3 & 12/17 & 12/17 & -1/3 & -443/2993 & -17/216 & 0 \\ \hline & 13/102 & -1/3 & 12/17 & 12/17 & -1/3 & 13/102 & 0 & 0 \end{array} \tag{14}$$

This 8-stage method looks very computationally expensive. Notice, however, that the last two stages are equal to the fifth and forth stages, respectively, and that the first three stages are explicit. Hence, the product

$$Y_{\text{tmp},1} = \exp\left(\tfrac{12}{17}hF_{Y_3}\right)\exp\left(-\tfrac{1}{3}hF_{Y_2}\right)\exp\left(\tfrac{13}{102}hF_{Y_1}\right)y_n$$

should be computed only once in each step, regardless of the number of iterations the implicit method needs in order to converge. In addition, we see that the first five elements in rows four to six are the same, hence we need computing

$$Y_{\text{tmp},2} = \exp\left(-\tfrac{1}{3}hF_{Y_5}\right)\exp\left(\tfrac{12}{17}hF_{Y_4}\right)Y_{\text{tmp},1}$$

only once during each iteration.

In the next section we turn to numerical examples.

3 Numerical Simulations

3.1 The Heavy Top Equation

In this section we test the numerical methods on the equations for a rigid body under the influence of gravity. This set of equations can be modeled with the configuration space $\mathrm{SE}(3)$, with the dynamic variables evolving in the dual Lie algebra $\mathfrak{se}(3)^*$. Further, this is a Hamiltonian system where we use the coadjoint action to update the dynamic variables during the integration. Let $\mathbf{\Pi} \in \mathfrak{so}(3)^*$ be the angular momentum and $\mathbf{\Gamma} \in \mathfrak{so}(3)$ the gravity vector as seen in local coordinates. The heavy top equations are then

$$\begin{aligned} \frac{\mathrm{d}\mathbf{\Pi}}{\mathrm{d}t} &= \mathbf{\Pi}\times\mathbf{\Omega} + Mgl\mathbf{\Gamma}\times\boldsymbol{\chi}, \\ \frac{\mathrm{d}\mathbf{\Gamma}}{\mathrm{d}t} &= \mathbf{\Gamma}\times\mathbf{\Omega}, \end{aligned} \tag{15}$$

where $\mathbf{\Omega} = \mathrm{I}^{-1}\mathbf{\Pi}$ is the angular velocity of the top, I denotes the inertia tensor, $\boldsymbol{\chi}$ is the constant unit vector along the line segment of length l connecting the fixed point (origin) and the center of gravity of the top. M is the mass of the top, and g is the gravitational constant. We refer to [11] for background and notation.

The system (15) possesses four first integrals in the case of a symmetric top. These are the Hamiltonian, $\mathrm{H}(\mathbf{\Pi},\mathbf{\Gamma}) = \frac{1}{2}\mathbf{\Pi}\cdot\mathrm{I}^{-1}\mathbf{\Pi} + Mgl\,\mathbf{\Gamma}\cdot\boldsymbol{\chi}$, the projection of the angular momentum on the symmetry axis of the top $\mathbf{\Pi}\cdot\boldsymbol{\chi}$, the projection of the angular momentum on the gravity vector $\mathbf{\Pi}\cdot\mathbf{\Gamma}$, and the norm of the gravity vector $\|\mathbf{\Gamma}\|^2$. The two latter first integrals are Casimirs of the Poisson bracket defining the Hamiltonian structure.

The system (15) has been simulated with the following data (see [5, 15, 4]):

$$\mathrm{I} = \frac{1}{8}\begin{bmatrix} 7 & 0 & 0 \\ 0 & 7 & 0 \\ 0 & 0 & 2 \end{bmatrix}, \quad \boldsymbol{\chi} = \begin{bmatrix} 0 \\ 0 \\ 1 \end{bmatrix},$$

and

$$\mathbf{\Pi}_0 = \begin{bmatrix} 0 \\ 0 \\ 0.25 \end{bmatrix}, \quad \mathbf{\Gamma}_0 = \begin{bmatrix} 0 \\ -0.195090 \\ 0.980785 \end{bmatrix}.$$

Moreover, the gravitational constant g equals 9.81, the length l equals $\frac{\sqrt{3}}{2}$, and the mass M equals 1. The stepsize of the integration was $h = 0.05$, while the interval of integration was $[0, 25]$.

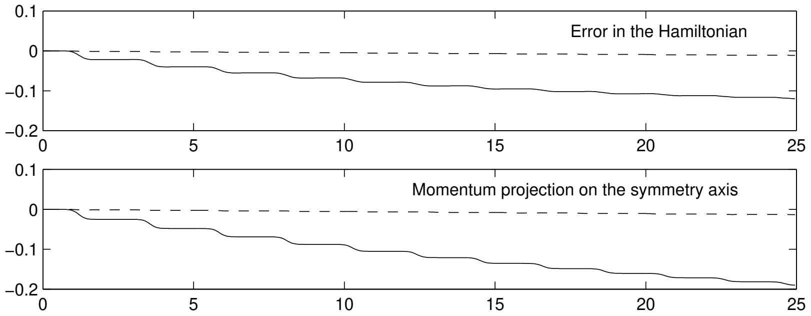

Figure 2: Non-Casimir first integrals of the heavy top equation integrated using the Crouch–Grossman method. Solid line: coefficients **CG3a**, broken line: coefficients **CG4**.

Figure 2 shows how well the Crouch–Grossman method with **CG3a** and **CG4** coefficients render the two non-Casimir first integrals of the heavy top. As we can see there is a significant drift in the results for both integrals, and for both methods. The Casimirs are preserved to machine accuracy by the coadjoint action, and, hence, not plotted.

Figure 3 shows the results for the symmetric Crouch–Grossman procedure as specified in Section 2.1, and Figure 4 shows the results for the symmetric Crouch–Grossman method (14). Both methods display a good behavior with respect to the retention of the two non-Casimir first integrals. The errors are oscillating within a constant band, and are not increasing with time. In Figure 5 the method (14) is used to integrate the equations with time-step $h = 0.2$ over the inteval $[0, 100]$. Notice that the error in the Hamiltonian is confined within a band. The overall behavior of the numerical Hamiltonian is as expected: preserved to within an upper and lower constant limit.

3.2 The Sine–Euler Equation

It can be shown that the 2D Euler equation of ideal fluid flow constitute an infinite dimensional Hamiltonian system [1]. One way of attacking this problem numerically is to truncate the original system of equations to a finite size model inheriting the features of the original Hamiltonian system. This was done in [16], and this truncated set of equations is called the Sine–Euler equation:

$$\dot{\omega}_{\mathbf{m}}(t) = \sum_{\substack{\mathbf{k}=-\infty \\ (k_1,k_2)\neq(0,0)}}^{\infty} \frac{\mathbf{m} * \mathbf{k}}{|\mathbf{k}|^2} \omega_{\mathbf{m}+\mathbf{k}} \omega_{-\mathbf{k}}, \qquad \mathbf{m} = (m_1, m_2) \in \mathbb{Z}^2, \tag{16}$$

where $\mathbf{k} = (k_1, k_2)$, $\mathbf{m} * \mathbf{k} = m_1 k_2 - m_2 k_1$ and $\omega_{\mathbf{m}}$ are the Fourier coefficients. In the following we consider the case where the dimension is 3. We work on the Lie algebra $\mathfrak{su}(3, \mathbb{C})$, which is of

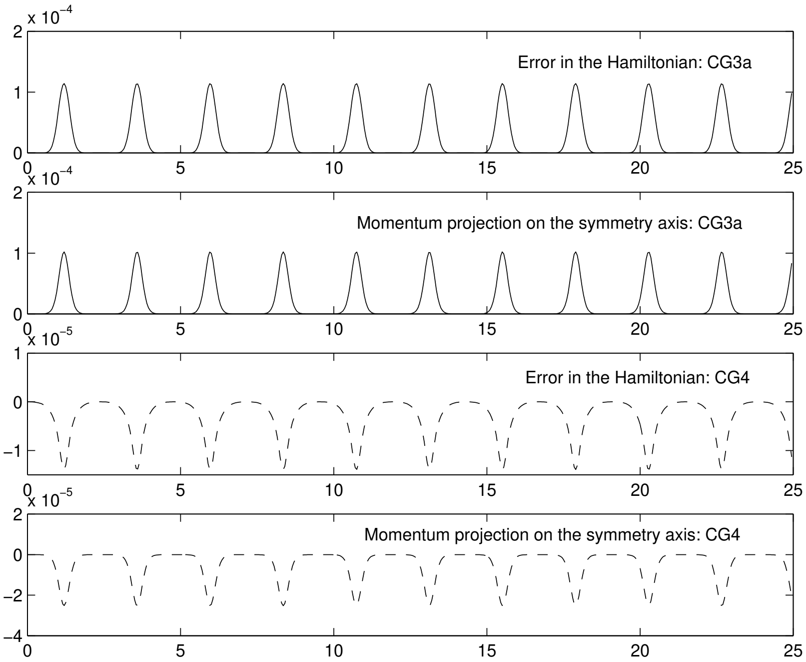

Figure 3: Non-Casimir first integrals of the heavy top equation integrated using the symmetric Crouch–Grossman procedure from Section 2.1. Solid line: coefficients **CG3a**, broken line: coefficients **CG4**.

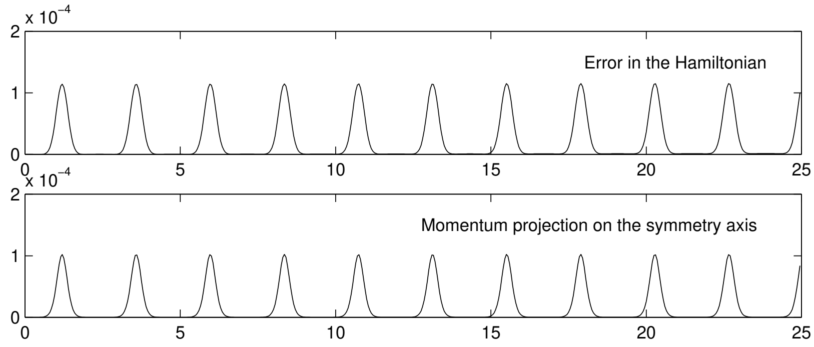

Figure 4: Non-Casimir first integrals of the heavy top equation integrated using the symmetric Crouch–Grossman method (14).

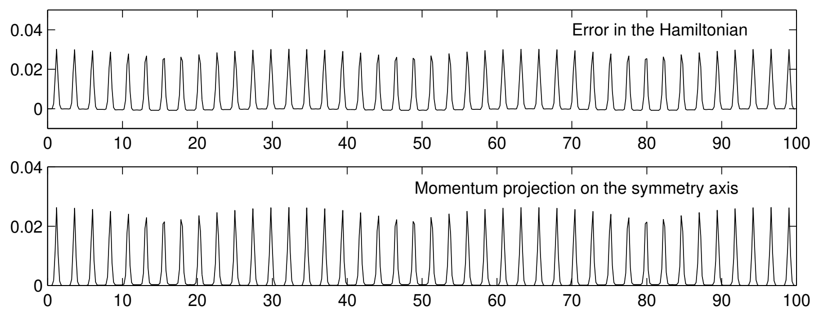

Figure 5: Non-Casimir first integrals of the heavy top equation integrated using the symmetric Crouch–Grossman method (14) with timestep $h = 0.2$.

dimension 4. It is now possible to reduce equation (16) to the following simple form:

$$
\begin{aligned}
\dot{\omega}_1(t) &= \frac{\sqrt{3}}{4}\,(\omega_2\omega_3^* - \omega_3\omega_4^*)\\
\dot{\omega}_2(t) &= \frac{\sqrt{3}}{4}\,(\omega_3^*\omega_4^* - \omega_4\omega_1^*)\\
\dot{\omega}_3(t) &= \frac{\sqrt{3}}{4}\,(\omega_1\omega_4 - \omega_1^*\omega_2)\\
\dot{\omega}_4(t) &= \frac{\sqrt{3}}{4}\,(\omega_1\omega_2 - \omega_2^*\omega_3^*)\,,
\end{aligned}
$$

where * denotes complex conjugation. This system has three first integrals: two quadratic and one cubic. The two quadratic first integrals are the Hamiltonian

$$H(\omega) = \frac{1}{2}\sum_{\mathbf{m}=-\infty}^{\infty} \frac{\omega_{\mathbf{m}}\omega_{-\mathbf{m}}}{|\mathbf{m}|^2}$$

and the Casimir

$$C_1 = \sum_{\mathbf{k}\in C} \omega_{\mathbf{k}}\omega_{-\mathbf{k}},$$

where C is the so-called fundamental cell around the origin of the frequency spectrum. The cubic first integral is the Casimir

$$C_2 = \sum_{\mathbf{m},\mathbf{k}\in C} \cos\left(\frac{2\pi}{3}(\mathbf{k} * \mathbf{m})\right)\omega_{\mathbf{k}}\omega_{\mathbf{m}}\omega_{-\mathbf{k}-\mathbf{m}}.$$

For more details, see e.g. [1, 16]. For numerical experiments of the Sine–Euler system with the Runge–Kutta–Munthe-Kaas method, see [3].

We have solved the system with a random and complex initial vorticity distribution and used the constant step size $h = 0.05$. The numerical methods are the original Crouch–Grossman method, the symmetric Crouch–Grossman method obtained by integrating half a step with the Crouch–Grossman

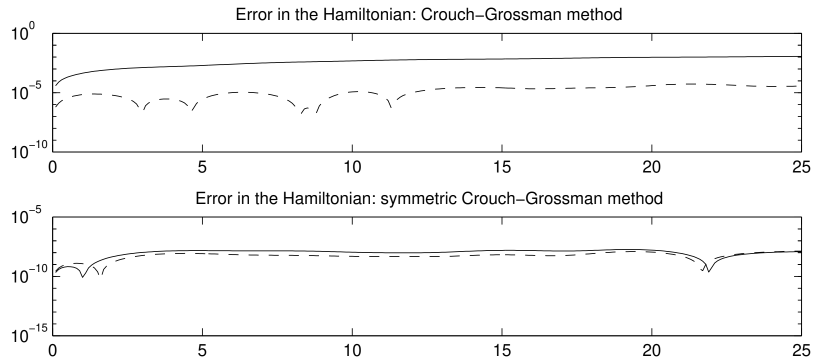

Figure 6: Error in the Sine–Euler Hamiltonian. The upper figure shows the error in the Hamiltonian when using the Crouch–Grossman method. The lower figure shows the error when using the symmetric Crouch–Grossman method from Section 2.1. Solid line: coefficients **CG3a**, broken line: coefficients **CG4**.

method and half a step with its adjoint, as described in Section 2.1, and the self-adjoint Crouch–Grossman method (14). The coefficients used are **CG3a** from [14] and **CG4** and **CG5a** from [10]. Again, we do not plot the Casimirs, since they are preserved to machine accuracy.

Figure 6 shows the results for the Crouch–Grossman method and the symmetric Crouch–Grossman method of Section 2.1. The error in the Hamiltonian does not have a regular behavior, and the oscillations have an irregular amplitude and period. However, in the upper subplot one can see that despite the irregularity, there is a linear drift. In the lower plot there is no tendency of drift, hence the symmetric method improve on the retention of the Sine–Euler Hamiltonian.

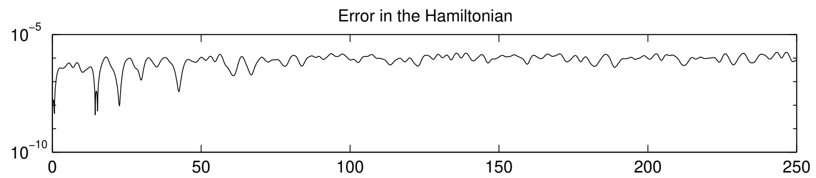

Figure 7: Error in the Sine–Euler Hamiltonian integrated with the symmetric Crouch–Grossman method (14) over the interval $(0, 250)$.

In Figure 7 we have integrated the Sine–Euler equations over a longer period of time, in order to check that there is no drift in the Hamiltonian error over time.

4 Concluding Remarks

In this paper we have discussed time-symmetry of the Crouch–Grossman class of geometric integrators. We found a representation of the adjoint Crouch–Grossman method as a $2s - 1$ stage Crouch–Grossman method, and numerical experiments support that this is a correct interpretation of the adjoint method. The reason for the increase in the number of stages in the adjoint Crouch–Grossman method, is non-commutative effects. We have also found examples of higher-order symmetric Crouch–Grossman methods.

Acknowledgment

We thank Hans Munthe-Kaas for valuable discussions related to the present work.

References

[1] V. I. ARNOLD AND B. A. KHESIN, *Topological Methods in Hydrodynamics*, Springer-Verlag, 1998.

[2] P. E. CROUCH AND R. GROSSMAN, *Numerical Integration of Ordinary Differential Equations on Manifolds*, J. Nonlinear Sci., 3 (1993), pp. 1–33.

[3] K. ENGØ AND S. FALTINSEN, *Numerical Integration of Lie–Poisson Systems while Preserving Coadjoint Orbits and Energy*, Tech. Rep. No. 179, Department of Informatics, University of Bergen, 1999.

[4] K. ENGØ AND A. MARTHINSEN, *A Note on the Numerical Solution of the Heavy Top Equations*. To appear in Multibody System Dynamics.

[5] ——, *Modeling and Solution of Some Mechanical Problems on Lie Groups*, Multibody System Dynamics, 2 (1998), pp. 71–88.

[6] S. FALTINSEN, *Backward Error Analysis for Lie–Group Methods*, Tech. Rep. 1998/NA12, Department of Applied Mathematics and Theoretical Physics, University of Cambridge, England, 1998.

[7] E. HAIRER, *Numerical Geometric Integration*. Downloaded from `http://www.unige.ch/math/folks/hairer/`, March 1999.

[8] E. HAIRER, S. P. NØRSETT, AND G. WANNER, *Solving Ordinary Differential Equations I, Nonstiff Problems*, Springer-Verlag, second revised ed., 1993.

[9] A. ISERLES, S. P. NØRSETT, AND A. F. RASMUSSEN, *Time-Symmetry and High-Order Magnus Methods*, Tech. Rep. 1998/NA06, Department of Applied Mathematics and Theoretical Physics, University of Cambridge, England, 1998.

[10] Z. JACKIEWICZ, A. MARTHINSEN, AND B. OWREN, *Construction of Runge–Kutta Methods of Crouch–Grossman Type of High Order*, Tech. Rep. Numerics No. 4/1999, The Norwegian University of Science and Technology, Trondheim, Norway, 1999.

[11] J. E. MARSDEN AND T. S. RATIU, *Introduction to Mechanics and Symmetry*, no. 17 in Texts in Applied Mathematics, Springer-Verlag, second ed., 1999.

[12] A. MARTHINSEN, *Interpolation in Lie Groups*, SIAM J. Numer. Anal., 37 (1999), pp. 269–285.

[13] H. MUNTHE-KAAS AND B. OWREN, *Computations in a Free Lie Algebra*, Phil. Trans Royal Soc. A, 357 (1999), pp. 957–981.

[14] B. OWREN AND A. MARTHINSEN, *Runge–Kutta Methods Adapted to Manifolds and Based on Rigid Frames*, BIT, 39 (1999), pp. 116–142.

[15] A. ZANNA, K. ENGØ, AND H. Z. MUNTHE-KAAS, *Adjoint and Selfadjoint Lie–Group Methods*, Tech. Rep. 1999/NA02, Department of Applied Mathematics and Theoretical Physics, University of Cambridge, England, 1999.

[16] V. ZEITLIN, *Finite-Mode Analogs of 2D Ideal Hydrodynamics: Coadjoint Orbits and Local Canonical Structure*, Physica D, 49 (1991), pp. 353–362.